Polym. Bull. (2012) 68:37–51
DOI 10.1007/s00289-011-0517-9

ORIGINAL PAPER

Synthesis and characterization of poly(methyl methacrylate-butyl acrylate) by using glow-discharge electrolysis plasma

Jinzhang Gao · Xingfa Li · Quanfang Lu · Yan Li · Deli Ma · Wu Yang

Received: 28 December 2010 / Revised: 18 May 2011 / Accepted: 22 May 2011 /
Published online: 27 May 2011

Abstract A highly absorptive resin was prepared by glow-discharge electrolysis plasma initiated suspension copolymerization, in which methyl methacrylate and butyl acrylate were used as monomers, *N*,*N*′-methylenebis(acrylamide) as cross-linking agent, polyvinyl alcohol as dispersant, and Na_2SO_4 solution as supporting electrolyte. To optimize the synthesis conditions, the discharge voltage, discharge time, polymerization temperature, the ratio of monomers, the amounts of cross-linking agent and supporting electrolyte, as well as the ratio of water to oil, were examined in detail. The structure and properties of the obtained resin were characterized by means of attenuated total reflectance Fourier transform infrared spectroscopy (ATR FT-IR), thermogravimetric analysis (TG), differential scanning calorimetry (DSC), and scanning electron microscopy (SEM), respectively. The oil absorbency, absorption rate, absorption selectivity, and network parameters of the resin were also examined. Results showed that under the optimal conditions, the oil absorbency was about 28.5 g/g for benzene, 25.4 g/g for toluene, 28.0 g/g for xylene, 38.1 g/g for chloroform, and 37.0 g/g for carbon tetrachloride.

Keywords Glow-discharge electrolysis plasma · Copolymerization · Acrylic resin · Absorption selectivity · Absorption kinetics · Network parameters

Introduction

Pollution of oil and oil-like organic solvents to water sources, such as ocean, river and lake, is one of the most calamities for human, animal, halobios, and plant. So far, there is no ideal technique for treating such contaminations. The application of

J. Gao (✉) · X. Li · Q. Lu · Y. Li · D. Ma · W. Yang
College of Chemistry & Chemical Engineering, Northwest Normal University, Lanzhou 730070, People's Republic of China
e-mail: jzgao@nwnu.edu.cn

the highly absorptive resin, perhaps, could catch a part of contaminations to decrease the pollution and recovery the solvents [1–3]. Recently, the acrylic resin has received a great deal of attention [4–6] due to its multiple oil-absorbent species, high oil absorbency, well oil retention and recoverability, especially, the use of green synthetic techniques.

Glow-discharge electrolysis is a kind of non-Faradaic electrochemical process, which occurs at solution surface or under aqueous solution as the applied voltage over a critical value. As there are many energetic species in the glow-discharge area like plasma, it is said to be the glow-discharge electrolysis plasma (GDEP). Based on the different position of electrodes, various terms were used. For example, if the anode was above solution (close to the solution surface), the discharge would be called "contact glow-discharge electrolysis" [7]; if both anode and cathode were placed in solution simultaneously, it would be called "submersed glow-discharge electrolysis plasma" [8], "glow-discharge electrolysis plasma under water" [9], or "glow-discharge electrolysis plasma under solution" [10]. In view of basic principle, they are the same, belonging to non-Faradaic electrolysis. In this work, we are fond of using the term "glow-discharge electrolysis plasma" (GDEP) to describe this plasma. GDEP can be considered as a rich source of free radicals to induce some unusual chemical reactions in aqueous solution [11]. As the plasma from GDEP can be used to initiate polymerization reaction in aqueous media without any initiator, catalyst, and organic solvent, so the pollution to environment will be decreased significantly. Compared with the high pressure and high vacuum apparatus used to produce plasma, this technique is rather cheap in cost for the setup and very easy in operation.

Although this technique has been used successfully in the wastewater treatment [12–15], the use in synthetic chemistry [16–19] seems to be in an approach stage. In this article, a highly absorptive resin was synthesized by suspension copolymerization, which was initiated via GDEP. Commonly, the term "oil" in many papers refers to all organic substances that are insoluble in water rather than only just to petroleum. Of course, the most used target "oil" in discussion is the organic solvents. Thus, some concepts concerning the oil-absorptive resin were also adopted in this study, for example, oil absorbency, solubility parameters, and so on. Several organic compounds (i.e., benzene, toluene, xylene, chloroform, and carbon tetrachloride) which were considered as contaminations (or called oil contaminations), were examined. The relationship between polymerization conditions and the oil absorbency were also discussed in detail.

Experimental

Reagents and apparatus

Chemicals used, such as methyl methacrylate (MMA), butyl acrylate (BA), *N*,*N*′-methylenebis(acrylamide) (MBA), polyvinyl alcohol 1750 ± 50 (PVA), sodium sulfate, sodium hydroxide, anhydrous magnesium sulfate, tetrahydrofuran (THF), benzene, toluene, xylene, chloroform, and carbon tetrachloride, were of

analytical reagent grade. MMA and BA were washed with 5% sodium hydroxide three times before use, and then washed with deionized water until neutralization. After being dried over anhydrous magnesium sulfate, the monomers were distilled twice under reduced pressure.

The experimental apparatus was similar to the one described in references [17, 18], consisting of a high voltage power supply and a reactor. The power supply was a Model of LW100J1 DC power supply providing the voltage of 0–1000 V and current of 0–1 A. The reactor was a 250 mL four-necked flask equipped with a reflux condenser, a nitrogen conduit, a platinum anode with a diameter of 0.5 mm sealed into a glass tube to generate glow-discharge plasma in aqueous solution and a graphite cathode with a diameter of 10 mm. The platinum wire out of the glass tube was about 3 mm. The anode and cathode were immersed simultaneously into solution, and the distance between two electrodes was about 3 cm. There was a magnetic stirring bar at the bottom of the flask to keep the solution mixed well. The flask was placed on a temperature-controlled oil bath.

The attenuated total reflectance Fourier transform infrared (ATR FT-IR) spectra were collected by using a Nicolet NEXUS 670 FT-IR single-beam spectrometer (USA) with a 4 cm^{-1} resolution and a 45° angle maintaining constant contact pressure between the Ge crystal and the specimens. Thermal stability measurements were performed on a Mettler Toledo TG/DSC-1 apparatus (Switzerland) from 30 to 800 °C, with a heating rate of 10 °C/min under a nitrogen flow rate of 50 mL/min. The morphological analyses were carried out through a scanning electron microscopy (SEM) (model: JSM-5600LV, Japan), using an applied voltage of 20 kV. Before SEM observation, all samples were fixed on copper stubs and coated with gold.

Preparation of highly absorptive resin

A typical experiment described as follows. A mixture containing 2 mL of 0.8% PVA aqueous solution, 18 mL of 2 g/L Na_2SO_4 solution, 0.03 g of MBA, 10 mL of MMA, 20 mL of BA was first added into a four-necked flask. Then, the mixture was stirred at 30 °C for 30 min to disperse homogeneously, while nitrogen was also bubbled to remove oxygen. The glow discharge was carried out for 12 min with an applied voltage of 600 V and current of 50–70 mA according to the desired parameters in advance. After rising the temperature of oil bath to 80 °C to react for 10 h under N_2 ambient, the polymerization reaction was continued for additional 30 min at 85 °C. The product was washed with warm-distilled water (ca. 70 °C) for several times, and then, dried under vacuum at 60 °C until a constant weight.

Performance tests

Oil absorbency

Oil absorbency (*W*, g/g) was determined at 298 K through ASTM (F726-06): An accurately weighed sample was immersed in excess solvent at room temperature to

reach swelling equilibrium. Then, the sample was filtered and immediately weighed. The oil absorbency was calculated by the following equation:

$$W = \frac{m - m_0}{m_0},$$

where m_0 (g) and m (g) are the weights of the dry sample and the swollen sample, respectively.

Absorption rate

An accurately weighed sample was immersed in excess solvent at room temperature. After 1 h, the sample was took out to peel off the un-absorbed solvent and then weighed. The above operation was repeated for eight times to ensure the equilibrium completely. Of course, the determination of absorption rate may be measured by the different interval times.

Results and discussions

Optimization of polymerization conditions

Effects of discharge voltage on oil absorbency

Discharge voltage has critical influence on the polymerization, since the free radicals generated by GDEP is equivalent to the chemical initiator in the polymerization reaction. As the lower discharge voltage used, polymerization hardly occurred, because the amount of free radicals was too poor, and life expectancy of them very short. With the rising of applied voltage, the energetic species including radical increased, a well three-dimensional network structure was effectively formed, and the oil absorbency increased (see Fig. 1a). However, the excess of free radical could also destroy the resulted polymer [18, 19]. In addition, the reactants would be carbonized, even the platinum anode would be molten under the strong glow discharge. For the same reason, the discharge time should be controlled within a suitable range.

Effect of polymerization temperature on oil absorbency

It can be seen from Fig. 1b, as the polymerization temperature rising, effective collisions between energetic species and monomers increased, the polymerization rate would speed up. Below 70 °C, the reaction is very slow. Over 80 °C, the polymerization and chain propagation rate greatly accelerated to cause easily the product agglomerate. If the temperature still increases up to 90 °C, a saddle-type in oil absorbency appear, maybe, causing by the evaporation of water and the shrinkage of resin. After that, the physical absorption could take place.

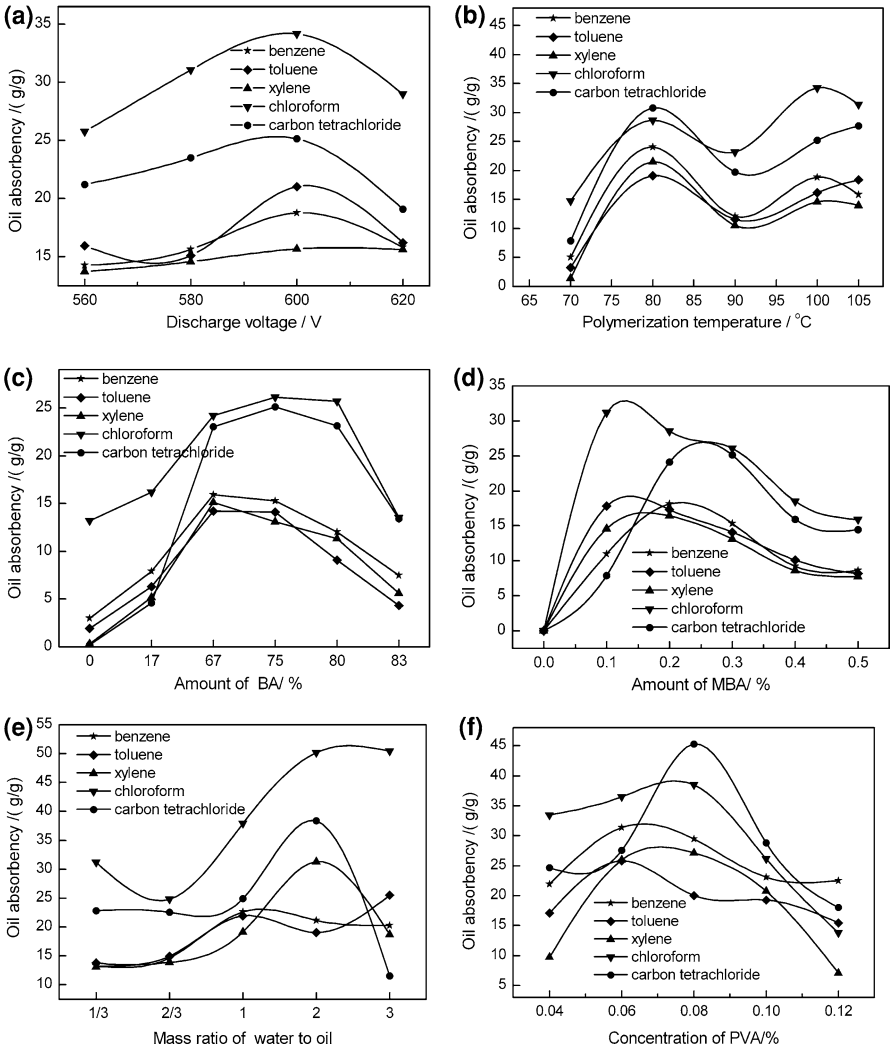

Fig. 1 **a** Effect of discharge voltage, **b** effect of polymerization temperature, **c** effect of monomer BA content, **d** effect of MBA content, **e** effect of ratio of water to oil, and **f** Effect of PVA concentration

Effect of monomer BA content on oil absorbency

The low oil absorbency appeared at the low content BA in the comonomer. The short carbon chain in MMA ester group would decrease the lipophilicity of resin, meanwhile increase the rigidity of resin. The excess of BA used can also reduce the rigidity of resin to decrease the oil absorbency. For improving the lipophilicity and rigidity, it is necessary to choose a suitable amount of BA in comonomer, just as shown in Fig. 1c.

Effect of MBA content on oil absorbency

In general, the used amounts of crosslinking agent determine the crosslinking density of resin. The linear resin dissolves easily in organic solvents without swelling, whereas the network resin can swell after oil absorbency due to the presence of network. Such property was related to the used amount of MBA. Just as shown in Fig. 1d, if the amount of MBA was not enough, a well three-dimensional network structure cannot form, leading to the oil absorbency declined. Contrarily, the excess of MBA will increase the crosslinking density and the rigidity, decreasing the swelling capability of resin.

Effect of ratio of the water/oil on oil absorbency

Figure 1e shows the effect of ratio of the water/oil on oil absorbency. If the lack of water were present, the larger droplets containing more monomers would not be benefit to polymerization; contrarily, the excess of water would prevent radicals from going into the droplets. Thus, a suitable ratio of the water/oil to be 2 was chosen in this work.

Effect of PVA concentration on oil absorbency

The dispersant used in the suspension polymerization system can reduce the surface tension of monomer phase, and prevent droplets from coalescing. Just as shown in Fig. 1f, if the amount of dispersant used was not enough, the resulting resin would harden to decrease the oil absorbency. Over a critical amount of PVA, for example, 0.08%, the oil absorbency will decline. Thereby, in this study, 0.08% of PVA was used as a suitable amount.

Infrared spectra analysis

The highly absorptive resin was first extracted with THF for 24 h in Soxhlet extractor and then dried in a vacuum drying oven before ATR-FTIR test. It can be seen from Fig. 2, a strong absorption peak at 1731 cm^{-1} is attributed to C=O stretching vibration, the absorption peaks at 1066 and 1164 cm^{-1} are assigned to C–O stretching vibration, and the absorption peak of C=C disappears. Such results imply the existence of polyester. The peaks appeared at 2958 and 2873 cm^{-1} are assigned to the $–CH_3$ asymmetric stretching vibration and symmetric stretching vibration, respectively. The absorptions appeared at 1454 and 1386 cm^{-1} are ascribed to $–CH_3$ antisymmetric bending vibration and symmetric bending vibration, respectively. The absorptions of 1238 and 1268 cm^{-1} are characteristic absorption peaks of PMMA. These peaks confirm the highly absorptive resin containing PMMA chains. The absorptions appeared at 940 and 960 cm^{-1} are butyl ester characteristic absorption peaks, indicate that the PBA chains exist in the resin. The wide peak appeared at 3444 cm^{-1} is attributed to the OH stretching vibration, which may be come from the PVA molecules residual in resin.

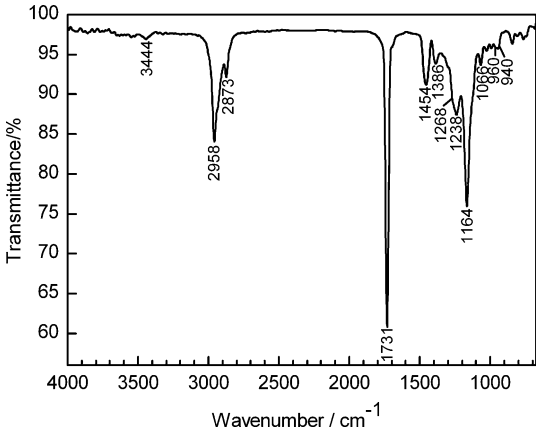

Fig. 2 ATP-FTIR spectra of the resin

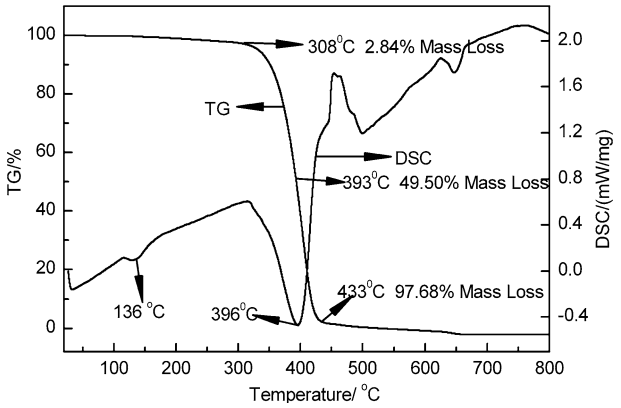

Fig. 3 The TG and DSC curves of the resin

Thermal stability analysis

It can be seen from Fig. 3, that the sample has a little of mass loss about 0.15% before 100 °C, this may be caused by evaporation of residual water in the resin. The rapid mass loss after 308 °C can emerge from the break of resin chain and decomposition of alkyl acrylate. It can be also learned from the DSC curve, the wide endothermic peak appeared between 115 and 165 °C, and the strong melting endothermic peak close to 396 °C are consistent with the water evaporation and resin decomposition. That is to say, the highly absorptive resin obtained has a good thermal stability, which can meet the need in many fields.

Morphology analysis

The scanning electron micrographs of the highly oil-absorptive resin were shown in Fig. 4. It can be seen that there are many deep holes in the surface and inside of the

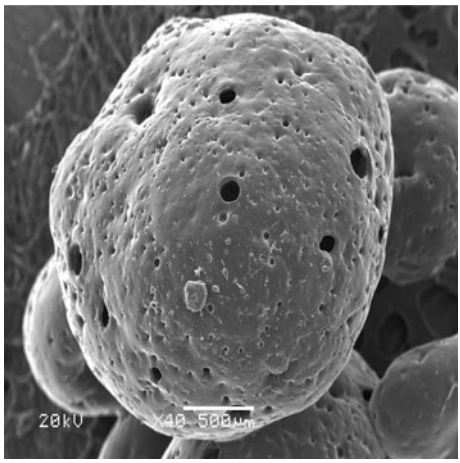

Fig. 4 SEM of the resin

resin. These holes can help oil spread into resin interior, working like a sponge. In addition, the oil cannot easily exude from the three-dimensional crosslinked resin.

Selectivity of absorption

Selectivity of absorption refers to the absorptive difference between organic solvent and water, and between organic solvents each other. For the former, the resin used must have high hydrophobicity and can float on the water. The acrylate resins can match such characteristics. In general, the latter, i.e., the absorptive difference between organic solvents each other, is a more important property for absorbents. Based on Flory's swelling theory, swelling behavior is affected by three factors, that is, the rubber elasticity, affinity to the solution, and crosslinking density. Affinity to the solution means that the selective absorption is related to the polarities and solubility parameters of the highly oil-absorptive resin and oils. As the highly oil-absorptive resin belongs to ester resin, with poor polarity, so has good affinity to non-polar solvents, which consistent with the principle of "like dissolves like" in aqueous chemistry. The polymer–solvent interaction parameter (χ) could be used to predict the absorptive selectivity, which was calculated from the solubility parameter of solvents, δ_1, and the networks, δ_2:

$$\chi = \frac{(\delta_1 - \delta_2)^2 V_1}{RT},$$

where R is the gas constant, T is the absolute temperature, and V_1 is the molar volume of solvent. The low value of χ means that the weak interaction of interchains, and the strong interaction between the resin and the solvent are existed. In other words, if the solubility parameters of resin were similar to these of solvent, the large absorption of resin to solvent would occur. The theoretical solubility parameter can be calculated based on the structural formula of resin followed by the equation $\delta = \frac{F}{V_m} = \frac{\Sigma F_i}{\Sigma V_i}$, where δ ($(\text{MPa})^{1/2}$) is the solubility parameter, F ($(\text{J cm}^3)^{1/2}/\text{mol}$) is the molar-

attraction constant, V_m (cm^3/mol) is the molar volume, F_i ((J cm^3)$^{1/2}$/mol) and V_i (cm^3/mol) stand for the contribution from the individual atoms and the atomic groups to the molar-attraction constant and the molar volume, respectively. In this study, the structural formula of the resin can be considered as 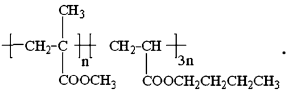 . The values of F_i and V_i for two atomic groups are listed in Table 1. Then, the value of δ can be calculated as follows:

$$\delta = \frac{F}{V_m} = \frac{\Sigma F_i}{\Sigma V_i} = \frac{1609.5 \times 1 + 2223.6 \times 3}{81.9 \times 1 + 114.9 \times 3} = 19.4$$

According to the theoretical solubility parameter, several organic compounds with the approximated solubility parameters were chose to the tested solvents. It can be seen from Table 2, the obtained resin has higher oil absorbency to all tested solvents.

Based on the above representation, 16 solvents were chosen for studying the absorption. And the theoretical solubility parameters were used to calculate the polymer–solvent interaction parameter.

It can be seen from Table 3, the solvents with lower polarity (P) and lower polymer–solvent interaction parameter have larger oil absorbency, and vice versa. In other words, the polymer–solvent interaction parameter was associated with the structural formula and proportion of monomers, implying that for a given solvent, a directional synthesis can be reached from choosing the proper monomer and controlling the proportion.

Absorption rate and absorption kinetics

It can be seen from Fig. 5, the oil absorbency increased rapidly at the beginning due to the solvation of the network chains; the main driving force of this process is the change in the free energies of mixing and elastic deformation. However, the swelling is limited, that is, with time the absorption rate becomes slow and finally reaches saturation.

Table 1 F_i and V_i of atomic groups

Group	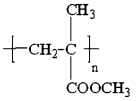		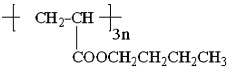	
	F_i [(J cm^3)$^{1/2}$/mol]	V_i (cm^3/mol)	F_i [(J cm^3)$^{1/2}$/mol]	V_i (cm^3/mol)
$-CH_3$	606.8	67	303.4	33.5
$-CH_2-$	269	16.1	1076	64.4
$-CH<$	0	0	176	−1
$>C<$	65.5	−19.2	0	0
–COO–	668.2	18	668.2	18
$\sum$	1609.5	81.9	2223.6	114.9

Table 2 Oil absorbency

Solvents	Benzene	Toluene	Xylene	Chloroform	Carbon tetrachloride
Oil absorbency (g/g)	28.5	25.4	28.0	38.1	37.0

Table 3 Polymer–solvent interaction parameter and oil absorbency

Solvents	P	χ	W (g/g)	Q (cm^3/g)
Dichloromethane	0.120	0.004	38.6	29.1
Chloroform	0.017	0.005	38.1	25.7
Benzene	0	0.018	28.5	32.5
Ethyl acetate	0.167	0.025	19.6	21.8
Tetrahydrofuran	0	0.027	25.3	28.4
Acetone	0.695	0.036	15.7	19.9
Xylene	0.001	0.049	28.0	32.8
Toluene	0.001	0.062	25.4	29.2
Carbon tetrachloride	0	0.126	37.0	23.2
Acetonitrile	0.852	0.505	8.9	11.3
Propyl alcohol	0.152	0.723	1.4	1.7
Methanoic acid		1.024	0.7	0.6
Ethanol	0.268	1.027	2.7	3.4
Methanol	0.388	1.733	0.5	0.6
Dimethyl sulfoxide	0.813	1.842	0.3	0.3
Water	0.819	5.662	0.3	0.3

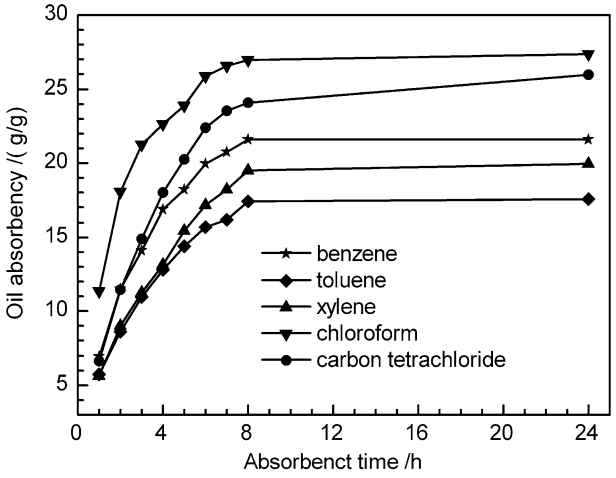

Fig. 5 Absorption rate

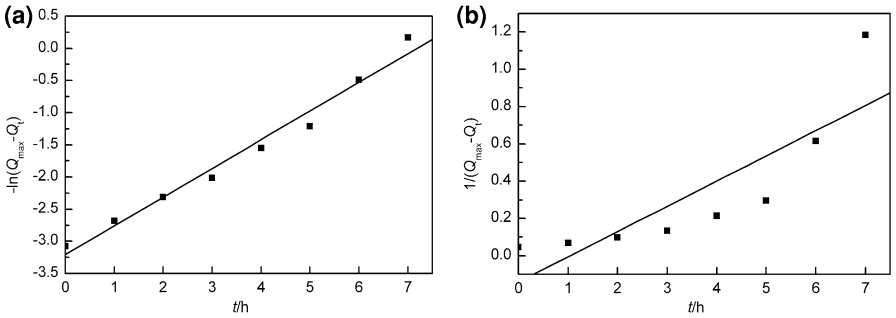

Fig. 6 **a** First-order absorption kinetics model and **b** second-order absorption kinetics model

In order to study the absorption kinetic process, benzene was selected as an example. Here, $Q_{\max}$ and Q_t are the maximum oil absorbency and the oil absorbency at time t, respectively. Assuming that the absorption kinetic process obeyed the first-order model

$$\frac{dQ}{dt} = k_1(Q_{\max} - Q_t) \tag{1}$$

Integration of Eq. 1

$$-\ln(Q_{\max} - Q_t) = k_1 t + c, \tag{2}$$

where k_1 is the absorption rate constant, c is the integration constant.

According to the Eq. 2, a plot of $-\ln(Q_{\max} - Q_t)$ against t with a straight line was obtained by the least square, showing in Fig. 6a.

Similarly, according to the second-order model

$$\frac{dQ}{dt} = k_2 (Q_{\max} - Q_t)^2 \tag{3}$$

Integration of Eq. 3

$$\frac{1}{Q_{\max} - Q_t} = k_2 t + c \tag{4}$$

A plot of $1/(Q_{\max} - Q_t)$ against t was obtained in Fig. 6b. k_1 and k_2 were calculated from the slopes to be 0.4459 and 0.1354, respectively. Clearly, the correlation coefficient for the first-order model ($R^2 = 0.9892$) is better than the second-order model ($R^2 = 0.8494$), indicating that first-order absorption kinetics was suitable to describe absorption rate.

Network studies

Absorptive capacity of the resin closely related to the network. Macroscopic properties of resin network include the resin density (ρ_p), Young's moduli of elasticity (E), the volume fraction of resin in swollen gel (Φ_p), and gel fraction (G). The values listed in Table 4 were measured at 293 K by using pure benzene as absorption medium. Data show that the densities of resins are always less than of

Table 4 Macroscopic properties of resin network

MMA (ml)	BA (ml)	MBA (%)	W (g/g)	ρ (kg/dm^3)	E (MPa)	Φ	G
20	10	0.2	10.0	0.95	118.5	0.085	75.7
15	15	0.2	15.4	0.88	0.82	0.061	75.0
10	20	0.1	24.0	0.63	0.24	0.055	79.2
10	20	0.2	20.3	0.71	0.27	0.057	93.6
10	20	0.3	14.2	0.77	0.29	0.074	94.9
10	20	0.4	8.0	0.99	0.48	0.100	71.3
10	20	0.5	7.8	0.97	0.59	0.104	72.5
7.5	22.5	0.2	13.6	0.88	0.10	0.068	97.2
5	25	0.2	24.0	0.66	0.05	0.052	89.5

water, indicating that the prepared resins in this work can float on water surface. In addition, with increasing the BA content, the density of the resin and its elastic modulus decrease. This is due to the MMA being the hard monomer, which would enhance the rigidity and Young modulus. However, BA can improve the flexibility and enable the resins to swell more easily; for example, with the increasing content of BA the value of volume fraction of resin in swollen decreases. Results show that the values for ρ_p and E increase with increasing MBA weight content. This is, perhaps, due to the decrease of probability of forming dangling chains or pendant groups as crosslinking agent increases. The presence of pendant chains or dangling chains in the network can affect the Young moduli. The values of moduli increase drastically when the proportion of pendant chains decrease [20]. The lower E value for crosslinked resins indicates that the prepared gels have elastic networks. This will increase interaction between benzene and networks, further, to increase the absorption capacity for crosslinked P(MMA-BA) resin.

The crosslinking degree of resin is expressed commonly by the term gel fraction, which was measured by an extraction method. A weighed filter paper bag with a weighed dried sample was put into a Soxhlet extractor on an oil bath at about 75 °C. The sample was extracted with THF for 24 h, and then the filter paper bag was weighed after drying at 70 °C. The G value was calculated according to the following equation: $G = \frac{G_b}{G_a} \times 100\%$, where G_a (g) and G_b (g) are weights of sample before and after extraction, respectively.

As the resin with lower gel fraction cannot form a complete three-dimensional network structure, the structure would be destroyed after absorbing solvents. That is to say, the resin would be intenerated. For balancing the rigidity and elasticity, the gel fraction should increase appropriately. Results show that gel fraction G increases with increasing the amount of crosslinking agent at first, and then, the excess of MBA cannot keep the gel fraction enhanced, indicating that the excess of crosslinking agent did not react to form the network.

Microscopic network parameters of the resin were also studied, as shown in Table 5, including the crosslink density (q), effective crosslink density (v_e),

Table 5 Network parameters of different compositions of resins

MMA (ml)	BA (ml)	MBA (%)	$v_e \times 10^3$ (mol/dm^3)	$M_c \times 10^{-3}$ (g/mol)	$q \times 10^3$ (mol/dm^3)	χ
20	10	0.2	36902.677	0.026	12757.061	0.01956
15	15	0.2	285.318	3.084	74.017	0.01654
10	20	0.1	86.409	7.291	48.891	0.01583
10	20	0.2	95.760	7.414	48.077	0.0158
10	20	0.3	94.304	8.165	43.656	0.01617
10	20	0.4	141.377	7.003	50.904	0.01607
10	20	0.5	171.702	5.649	63.098	0.01639
7.5	22.5	0.2	33.462	26.299	18.428	0.01623
5	25	0.2	18.266	36.133	20.507	0.01586

molecular weight of the chains between two successive crosslinks (M_c), and resin–solvent interaction parameter (χ). Based on Flory's swelling theory, v_e and M_c obtained from Eqs. 5 and 6 [21]:

$$\tau = RTv\Phi^{1/3}\left(\lambda - \lambda^{-2}\right) \tag{5}$$

$$G = \tau/\left(\lambda - \lambda^{-2}\right) = E/3 \tag{6}$$

$$v_e = E\Phi^{-1/3}/3RT \tag{7}$$

$$M_c = \rho_p/v_e, \tag{8}$$

where τ is the stress, λ is the ratio of the deformed length (L) of the resin to its undeformed length (L_0), G is the compression moduli of elasticity, respectively. The crosslink density q, is defined as the mole fraction of crosslinked units: $q=M_o/M_c$, where M_o is the molar mass of the repeating units. Polymer–solvent interaction parameter was calculated from the equation $\chi = \frac{(\delta_1-\delta_2)^2 V_1}{RT}$.

One of the important structural parameters for the crosslinked resins is M_c, which is directly related to the crosslink density. The magnitude of M_c significantly affects the physical and mechanical properties of the crosslinked copolymers and its determination has great practical significance [22]. Since M_c is used to determine the distance between two successive crosslinks, the smaller the value the higher the crosslinking density of the networks. Thus, M_c values decrease as crosslinker weight content increase, the reason may be that the increase in the amount of the crosslinking agent led to formation of a denser network. The values of q and v_e decrease with increasing the BA proportion in the resin composition, and increase with increasing the crosslinker weight content.

In this study, the values of χ are always <0.5 for the prepared resins swelling in benzene, implying that the resins have strong affinity with the benzene. The lower the values of χ, the higher the resin–solvent interaction are, and the larger the absorption capacity of resin. It can be also observed from Table 5 that the lower values of χ appeared at the higher BA, which may be attributed to the hydrophobic nature of the BA component.

Conclusion

In this article, a highly absorptive resin was successfully prepared by using GDEP initiated suspension polymerization. Results indicated that the high absorbency was relative to the low polarity of organic solvents and the approximate solubility parameter to the resin, and obeyed the first-order absorption kinetics. The hole-shape structure in surface of the resin can help improve oil-absorption behavior. Such excellent resin could expect to use in treatment of chemical pollution.

Acknowledgments This work was supported in part by the Key Project of Science and Technology of Education Ministry (00250), the Natural Science Foundation of Gansu Province (3ZS041-A25-028 and 096RJ2A120), the Project of KJCXGC-01, NWNU, and Gansu Key Lab of Polymer Materials, China.

References

1. Jang J, Kim BS (2000) Studies of crosslinked styrene-alkyl acrylate copolymers for oil absorbency application. II. Effects of polymerization conditions on oil absorbency. Appl Polym Sci 77:914–920
2. Li PX, Yu B, Wei XC (2004) Synthesis and characterization of a high oil-absorbing magnetic composite material. Appl Polym Sci 93:894–900
3. Zhou XM, Chuai CZ (2010) Synthesis and characterization of a novel high-oil-absorbing resin. J Appl Polym Sci 115:3321–3325
4. Atta AM, Arndt KF (2005) Swelling and network parameters of high oil-absorptive network based on 1-octene and isodecyl acrylate copolymers. J Appl Polym Sci 97:80–91
5. Atta AM, El-Ghazawy RAM, Farag RK (2006) Swelling and network parameters of oil sorbers based on alkyl acrylates and cinnamoyloxy ethyl methacrylate copolymers. J Polym Res 13:257–266
6. Farag RK, El-Saeed SM (2008) Synthesis and characterization of oil sorbers based on docosanyl acrylate and methacrylates copolymers. J Appl Polym Sci 109:3704–3713
7. Gao JZ, Wang XY, Hu ZA, Deng HL, Hou JG, Lu XQ, Kang JW (2003) Plasma degradation of dyes in water with contact glow discharge electrolysis. Water Res 37:267–272
8. Gao JZ, Pu LM, Yang W, Yu J, Li Y (2004) Oxidative degradation of nitrophenols in aqueous solution induced by plasma with submersed glow discharge electrolysis. Plasma Process Polym 1:171–176
9. Joshi R, Schulze R-D, Meyer-Plath A, Wagner MH (2009) Selective surface modification of polypropylene using underwater plasma technique or underwater capillary discharge. Plasma Process Polym 6:218–222
10. Yan ZC, Chen L, Wang HL (2006) Experimental study of plasma under-liquid electrolysis in hydrogen generation. Chin J Process Eng 6:396–400
11. Gao JZ, Wang AX, Fu Y, Wu JL (2008) Analysis of energetic species caused by contact glow discharge electrolysis in aqueous solution. Plasma Sci Technol 10:30–38
12. Gao JZ (2006) A novel technique for wastewater treatment by contact glow- discharge electrolysis. Pak J Biol Sci 9:323–329
13. Lu QF, Yu J, Gao JZ (2006) Degradation of 2,4-dichlorophenol by using glow discharge electrolysis. J Hazard Mater B 136:526–531
14. Gao JZ, Yu J, Li Y, He XY, Bo LL, Pu LM, Yang W, Lu QF, Yang ZM (2006) Decoloration of aqueous brilliant green by using glow discharge electrolysis. J Hazard Mater B 137:431–436
15. Gai K (2007) Plasma-induced degradation of diphenylamine in aqueous solution. J Hazard Mater 146:249–254
16. Sengupta SK, Sandhir U, Misra N (2001) A study on acrylamide polymerization by anodic contact glow-discharge electrolysis: A novel tool. J Polym Sci A 39:1584–1588
17. Gao JZ, Wang AX, Li Y, Fu Y, Wu JL, Wang YD, Wang YJ (2008) Synthesis and characterization of superabsorbent composite by using glow discharge electrolysis plasma. React Funct Polym 68:1377–1383

18. Wang AX, Gao JZ, Yuan L, Yang W (2009) Synthesis and characterization of polymethylmethacrylate by using glow discharge electrolysis plasma. Plasma Chem Plasma Process 29:387–398
19. Gao JZ, Wang YD, Yang W, Li Y (2010) Synthesis and characterization of adsorbent for Pb(II)-capture by using glow discharge electrolysis plasma. Bull Korean Chem Soc 31:406–414
20. Yokota K, Abe A, Hosaka S, Sakai I, Saito H (1978) A ^{13}C nuclear magnetic resonance study of covalently cross-linked gels. Effect of chemical composition, degree of cross-linking, and temperature to chain mobility. Macromolecules 11:95–100
21. Peppas NA, Merrill EW (1977) Crosslinked poly (vinyl alcohol) hydrogels as swollen elastic networks. J Appl Polym Sci 21:1763–1770
22. Erdener K, Dursun S, Yasemin C, Olgun G (2000) Swelling studies of copolymeric acrylamide/crotonic acid hydrogels as carriers for agricultural uses. Polym Adv Technol 11:59–68